Michael J. Flynn, PhD

Processing Digital Radiographs of Specific Body Parts[1]

For traditional screen-film radiographic systems, the radiation intensity transmitted through the subject is directly transformed to film opacity and displayed with an illuminator. The display characteristics of the acquired image cannot be altered. For digital radiographic systems, the recorded image is first stored temporarily as an array of raw image values. Computer processes then transform the raw data to image presentation values that can be used to print the image on film or to display the image on an electronic device (Fig 1). This display processing allows the characteristics of the image to be separately optimized for various views of each body part for which the system is used.

Display processing methods are essentially the same for all types of digital radiographic detectors. The detector first produces raw image values that have a simple, usually logarithmic relation to the input radiation intensity. Relatively complex display enhancement processes then modify these values to restore sharpness, reduce the appearance of quantum noise, and increase detail contrast. The modified data are mapped to presentation values that are used by a display device to generate the image. The specific processing methods used in current systems are described and discussed in this chapter.

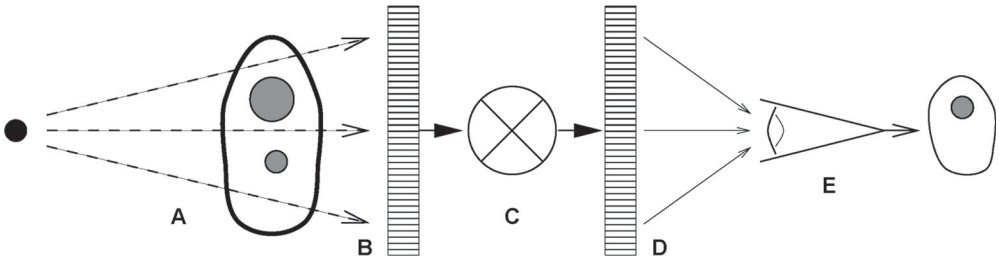

Figure 1. Five-component model of examination of patients with digital radiography. *A,* Generation of a beam of x rays incident on the patient and modulation of the x-ray beam intensity by tissue structures. *B,* Detection of the transmitted x-ray beam and creation of an array of raw image values (I_{raw}). *C,* Transformation of I_{raw} values to presentation values (I_p) with display processing. *D,* Display of the image with a standardized gray scale. *E,* Psychovisual interpretation of the displayed image by the observer.

Advances in Digital Radiography: RSNA Categorical Course in Diagnostic Radiology Physics 2003; pp 71–78.

[1]From Radiology Research, Henry Ford Health System, Suite 2F, 1 Ford Pl, Detroit, MI 48202 *(mikef@rad.hfh.edu).*

RAW IMAGE DATA VALUES

For most computed radiographic (CR) and flat-panel digital radiographic systems, the detector produces, at each image position, an electronic charge that is linearly proportional to the radiation energy absorbed at that position. At this stage of the system, the signal *(S)* is approximately proportional to the incident radiation exposure (E_{in}), as follows: $S = k_1 E_{in}$, where k_1 is a constant. This signal can be scaled such that it is equal to the noise equivalent number of x-ray quanta (NEQ) detected at each element of the image array (pixel): $I_{det} = k_2 S = Q_{eq}$, where I_{det} = detector signal, k_2 is a constant, and Q_{eq} = noise equivalent quanta. By convention, the noise in the signal (σ_{det}) is equal to the square root of the NEQ, as follows: $\sigma_{det} = Q_{eq}^{1/2}$. For negligible instrument noise, the NEQ is also proportional to the input exposure.

The preamplifier and digital converter of the system transform the charge to a voltage that is converted to a digital number representing the raw data image value (I_{raw}). Most systems transform the charge to a value proportional to the logarithm of the input exposure. This can be expressed in terms of the NEQ as follows: $I_{raw} = k_1 + k_2 \log_{10}(Q_{eq})$. The contrast of a particular structure that produces a fractional change in I_{det} of $e^{-\Delta\mu\Delta t}$ produces a change in the raw image value (ΔI_{raw}) that is independent of subject penetration and input exposure. For example, a system may transform input exposure to raw image values such that $I_{raw} = 2{,}000 + 1{,}000 \log_{10}(E_{in})$, where E_{in} is in milliroentgens. For this transformation, a raw image value of 1,000 results from an input exposure of 0.1 mR (0.258×10^{-4} mC/kg), the value of 2,000 results from 1 mR (0.258×10^{-3} mC/kg), and the value of 3,000 results from 10 mR (0.258×10^{-2} mC/kg). This transformation is convenient because a 10^4 range of input exposures can be expressed by using a 12-bit unsigned digital number ranging from 0 to 4,095.

Alternatively, one company has used a transformation such that the raw image values are proportional to the square root of the input exposure: $I_{raw} \cong 1{,}250 E_{in}^{1/2}$, or $I_{raw} = k\, Q_{eq}^{1/2}$. For transformations of this type, the quantum noise of I_{raw}, which is deduced from $\sigma_{raw}^2 = (dI_{raw}/dQ_{eq})^2\, \sigma_{det}^2$, does not vary with input exposure (1). This property is advantageous with respect to effective use of the limited image values of the digital converter. For logarithmic transformations, the quantum noise of I_{raw} varies with the inverse of the square root of the NEQ, and therefore the quantization of high signals is relatively coarse.

To date, no medical or industry standards exist to define the scale of numbers to be used for the raw image data of digital radiographs. Systems may use logarithmic or square root transformations, and different companies vary with respect to the constants used for the transformation. The wide variation in transformations used by different systems has hindered the introduction of image-processing methods that can be applied at a workstation to images from a variety of instruments. In this chapter, display processing is illustrated by using raw image data from a logarithmic transformation of the type described in the previous example.

GRAY-SCALE RENDITION

For each digital radiograph, the raw image data have a range of values that depends on the radiographic factors used (kilovolt peak, mAs, and filtration) and on the subject content (subject size, anatomic characteristics, body part, body position, and view). The highest values are typically found in regions outside of the subject, where the direct beam is recorded. If the exposure is collimated, the lowest values will be in regions outside of the collimator edges. Anatomic regions are distributed with values ranging between these limits (Fig 2).

In general, the gray-scale rendition maps the raw image values for the least penetrated anatomic region to the largest presentation value for display at maximum luminance. The most penetrated anatomic region of interest is mapped to the smallest presentation value for display at minimum luminance. The intermediate raw image values are then mapped to presentation values in a monotonically decreasing fashion. This produces a presentation with a black background similar to that of conventional radiographs.

For electronic presentation with a picture archiving and communication system (PACS) workstation, the raw image values may be sent along with DICOM (digital imaging and communications in medicine) header elements that indicate the minimum and maximum values of interest for presentation (ie, the value-of-interest [VOI] lookup table [LUT] window center and level elements) (2). The intermediate raw image values are mapped linearly to gray-scale presentation values. The observer can then adjust the range of values being presented to view regions of high or low penetrations or to increase contrast in a selected region.

To emphasize the contrast of intermediate raw image values, the values of I_{raw} are mapped to presentation values (I_p) by using a nonlinear relationship that emulates the Hurter and Driffield curve (H&D curve) familiar from screen-film radiography. The maximum and minimum raw image values are extended, and the intermediate values produce higher contrast than the extreme values. As with screen-film systems, the gray-scale rendition may have an extended toe or shoulder to extend contrast into anatomic regions with low or high penetration. The values of I_p are defined with the expectation that the luminance response of the display, $L(I_p)$, is calibrated to follow a standardized gray-scale display function (GSDF). For film printers, I_p is related to film density such that when the film is placed on a viewer, the brightness will follow the standard GSDF. The commonly used DICOM GSDF produces similar contrast perception over the full range of brightness (2).

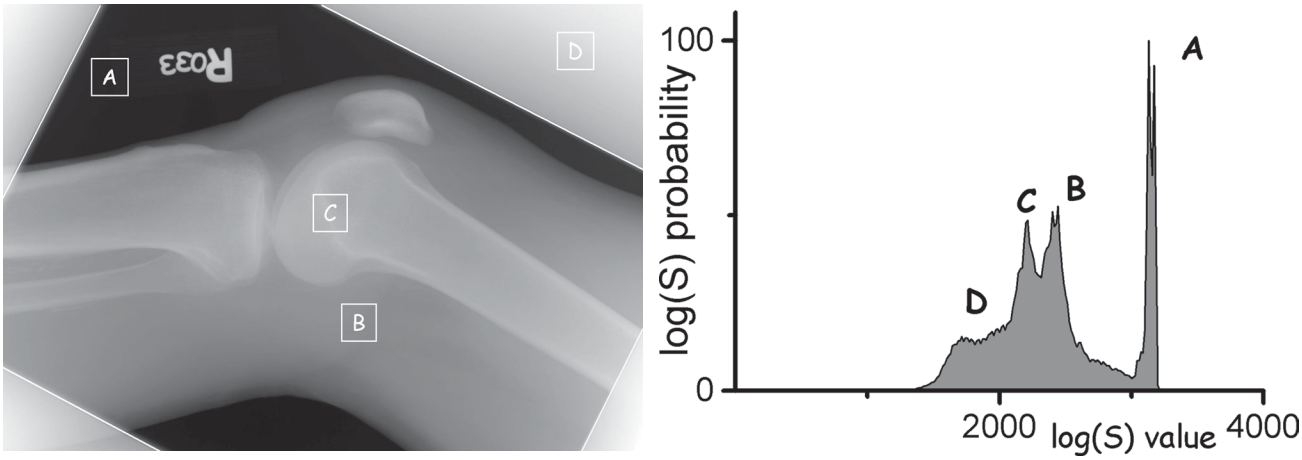

a. **b.**

Figure 2. **(a)** Commonly observed regions identified on an image of raw values (I_{raw}) from a knee radiograph: *A*, regions where the x-ray beam directly exposes the detector with no tissue attenuation; *B*, regions of modest tissue attenuation; *C*, regions of high attenuation from bone; and *D*, regions outside of the collimator edges exposed by scattered radiation. **(b)** Histogram of raw image values from a knee radiograph with commonly observed regions identified. *A*, Direct exposure produces a narrow peak of high values. *B*, Soft-tissue regions produce a broad peak of values less than those in *A*. *C*, Bone regions produce a broad peak of values less than those in *B*. *D*, Diffuse peak of low values outside the collimated region.

If image presentation values are sent to the workstation with a nonlinear gray scale already applied, the ability of the observer to make further adjustments of image contrast and brightness is severely limited. Instead, images can be sent to a PACS station as raw image values along with a gray-scale value-of-interest lookup table (ie, the VOI LUT sequence) (3). The display workstation can then stretch or compress the VOI LUT to adjust contrast, an operation analogous to adjusting the window width with linear presentation. Similarly, the VOI LUT can be translated to map higher or lower raw image values, an operation analogous to adjusting the window level.

EXPOSURE RECOGNITION

If the exposure to the receptor is unusually high or low, the histogram of I_{raw} values will be accordingly shifted. When I_{raw} is deduced from a logarithmic transformation, the shift occurs in a fixed amount for a fractional change. By using the previous example, if the exposure is doubled, the histogram shifts to the right by +301. If the exposure is reduced by a factor of 2, the histogram shifts to the left by −301. If the correct range of I_{raw} values can be identified for an individual acquisition, the gray-scale characteristics of displayed images will be the same when exposure variations shift the histogram. Exposure recognition processes are used to identify the minimum and maximum I_{raw} values to be used for the gray-scale rendition.

Exposure recognition processes typically segment the anatomic regions from areas that either *(a)* are outside the collimated region or *(b)* are regions recording the radiation beam directly with no tissue attenuation. Intelligent algorithms then identify the anatomic regions that should be displayed with either maximum or minimum brightness. Segmentation may be aided by examining the noise characteristics of the image values and by identifying structures that have straight edge characteristics (4–6). Complex rules may be used to refine the segmentation and reduce errors to less that 1% of the cases (7). Once segmented, the correct range of I_{raw} values is determined from the image values in the anatomic region. For views such as the posteroanterior chest, assumptions regarding the positions of the lung and the mediastinum can be used; however, more complex approaches are required in general (8). These exposure recognition processes are analogous to the automatic exposure-control systems used with modern photographic cameras. Like photographic camera products, many different approaches are employed for different digital radiographic products.

Although most exposure recognition processes work successfully for the majority of images recorded, occasionally the range of I_{raw} values is incorrectly deduced, and an unusually bright or dark image is presented. These errors often result from *(a)* unusually high radiation scatter, *(b)* unusual subject content, such as metal implants, or *(c)* interference from lead markers or holding devices. For the occasional exposure recognition failure, the technologist should be able to correct the processing at a quality control station. This correction is effectively done by using an application that can draw a region around the anatomic structures of interest and recompute the range of I_{raw} values.

Another function of the exposure recognition process is to estimate the average radiation exposure to the receptor in the anatomic regions of interest. This estimate is commonly reported to the operator as an index number that can be used to indicate whether

the proper radiographic technique was used. CR systems made by Fuji Medical Systems (Tokyo, Japan) report a number (S) that is inversely proportional to exposure.[2] CR systems made by Agfa Medical Systems (Ridgefield Park, NJ) report a number (lgM) that is proportional to the log of the exposure.[3] The lgM value varies with the user-selected speed. CR systems made by Eastman Kodak Company (Rochester, NY) report an exposure index (EI) proportional to the log of the exposure.[4] Similar values are reported for the digital radiographic systems made by Eastman Kodak Company. Unfortunately, there are no standards for the units that manufacturers use to report the exposure to the receptor, and the exposure index values used vary in both scale and direction in relation to exposure.

Because the exposure recognition process adjusts the gray scale to match the recorded range of I_{raw} values, the effects of excessive or insufficient exposure are not as readily apparent as they are for screen-film radiography. Insufficient exposure causes excessive quantum noise that can hinder interpretation. Excessive exposure causes high radiation dose to the patient and detector saturation but has no deleterious effect on image quality. Operators are thus instructed to maintain the exposure index within a specified target range. An index value that indicates insufficient exposure is a reason to repeat the radiographic image. An index value that indicates excessive exposure should be logged to determine if the technique factors should be systematically reduced. Because only low exposures are considered a cause to repeat a radiographic image, concern exists that exposure can "creep" to excessively high values (9).

EDGE RESTORATION

The x-ray projection through patient tissues that is recorded by a digital radiographic detector depicts fine detail with some blur. The blur can be due to the x-ray tube focal spot, patient motion, or the detector blur described by the modulation transfer function, MTF(f), of the instrument. Edge restoration processes are used to transform the blurred radiograph such that the fine detail reflects the actual characteristics of the tissue structures. Because the detector MTF(f) is generally the dominant source of blur, increasing the spatial frequencies in the recorded image in proportion to 1/MTF(f) can restore the actual spatial frequency content of the projected tissue structures. In practice, this process produces a large increase of the high-spatial-frequency content, which results in excessive amplification of quantum noise.

Edge restoration processes commonly assume that the radiographic system behaves like a linear system, with each projected ray through the patient being blurred in the detector by a characteristic point spread function that does not vary with image position. This assumption is good for the detector signal (I_{det}) but not for the nonlinear raw data values (I_{raw}). However, most tissue structures create modest variations in I_{raw} over the distances associated with the point spread function. In this case, the raw image values can be assumed to be locally linear with respect to image blur, local contrast, and noise. As an approximately linear system, the raw image values may be converted to an array of frequency-dependant Fourier coefficients, and the restoration may be effected by modification of the frequency coefficients by using a filter derived from the MTF(f). Alternatively, the restoration can be done by convolution with a kernel derived from the MTF(f).

To limit noise amplification, edge restoration filters may use a gain that is proportional to 1/MTF(f) only to amplify the image components with low and intermediate spatial frequencies. As frequency increases beyond the intermediate range, the filter function slowly returns to values of 1 or less. The Metz filter was developed for this purpose and has been shown to be effective in improving radiographic observer performance (10). The filter can be varied to control the amount of high-frequency gain permitted (11). Similar shapes can be obtained by modifying the inverse MTF(f) filter with a Butterworth filter that gradually diminishes coefficients above a specified frequency.

Edge restoration of this type can only be performed with knowledge of the MTF(f) for the detector system. Of particular importance is the reduction in modulation transfer that can occur at low and intermediate frequencies (ie, from about 0.1 to 0.5 of the limiting frequency associated with the spacing of the image values). For detectors that use scintillation phosphors, a simple model for the MTF(f) is given by the following expression: $\text{MTF}(f) = [1 - \exp(-a(f)]/a(f)$, where $a(f) = 1.6\, f/f_{1/2}$ (12), where f is the spatial frequency in cycles per millimeter, and $f_{1/2}$ is the spatial frequency for which the MTF(f) is equal to ½. For CR systems, this model overestimates the MTF(f) for values below 0.5 (13), which helps to avoid overamplification of high-frequency components. The model is useful in that it can be applied to high-resolution and regular CR screens as well as cesium iodide flat-panel detectors if the value of $f_{1/2}$ is known. For detectors that use photoconductors such as selenium, the MTF(f) is more appropriately described by the ideal response of a detector with square detector elements: $\text{MTF}(f) = \text{sinc}(\pi \Delta x f)$ (14).

When the edge restoration filter is appropriately specified, fine detail has a realistic appearance, and the image will not have excessive noise. This is illustrated in Figure 3 for a lateral knee view recorded with

[2]Fuji: $S = 200/E_{in}$ for an 80-kVp unfiltered beam.

[3]Agfa: $\text{lgM} = 2.22 + \log(E_{in}) + \log(S_n/200)$ for a 75-kVp beam with 1.5-mm Cu filtration, where S_n is the user-selected speed.

[4]Kodak: $\text{EI} = 1{,}000 \log(E_{in}) + 2{,}000$ for an 80-kVp beam with 0.5-mm Cu and 1.0-mm Al filtration.

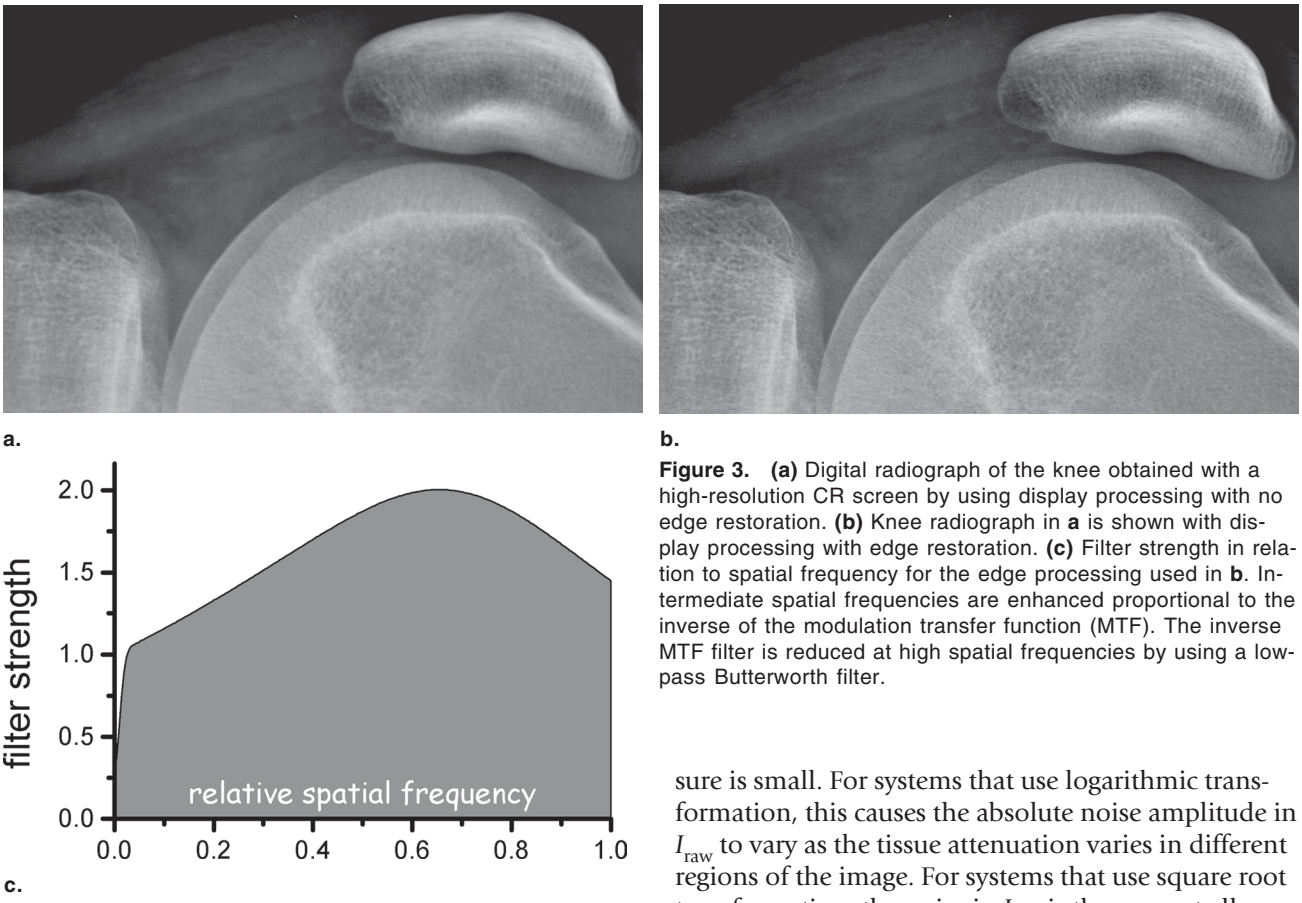

Figure 3. **(a)** Digital radiograph of the knee obtained with a high-resolution CR screen by using display processing with no edge restoration. **(b)** Knee radiograph in **a** is shown with display processing with edge restoration. **(c)** Filter strength in relation to spatial frequency for the edge processing used in **b**. Intermediate spatial frequencies are enhanced proportional to the inverse of the modulation transfer function (MTF). The inverse MTF filter is reduced at high spatial frequencies by using a low-pass Butterworth filter.

a CR system with a high-resolution phosphor screen. Inappropriate specification of the restoration filter can lead to artifacts. In some systems of earlier design, filters were implemented by using spatial convolutions based on a small kernel that were not able to amplify image components with low and intermediate spatial frequencies. These filters were often applied with excessively high gain. This overamplification of high spatial frequencies causes edge artifacts appearing as an oscillating signal that is sometimes referred to as "edge ringing."

NOISE REDUCTION

All digital radiographic devices are designed such that the only visible noise is due to the limited number of x rays detected per unit area. For photoconductive flat-panel devices, the quantum noise appears with a fine texture. The spatial frequency components of this noise are distributed with equal strength at all spatial frequencies; that is, the noise power spectrum, NPS(f), is constant in relation to frequency (14). For detectors that use scintillation phosphors (either CR or flat panel), the noise appears as a more nodular texture with the higher-frequency components somewhat diminished in strength (13). In both cases, the relative noise amplitude of I_{det} is large when the input exposure is small. For systems that use logarithmic transformation, this causes the absolute noise amplitude in I_{raw} to vary as the tissue attenuation varies in different regions of the image. For systems that use square root transformation, the noise in I_{raw} is the same at all positions in the image.

A variety of processing methods can be used to reduce the visual appearance of the noise texture. In general, these methods all reduce the high-frequency components associated with the noise signal, which results in a more nodular texture with reduced amplitude. As a consequence, these processes will also reduce the high-frequency components of the tissue signal, resulting in some blur. A general aim of noise reduction processes is to reduce the noise only in regions where the tissue contrast does not have noticeable fine detail.

If the frequency content of the tissue contrast is known along with the frequency content of the noise, the frequency-dependent contrast-to-noise ratio can be used to develop a noise reduction filter. The classical Wiener filter (15,16) provides an optimal solution that is based on the power spectrum of the tissue contrast signal, CPS(f), in relation to the noise power spectrum: $G(f) = 1/[1 + \mathrm{NPS}(f)/\mathrm{CPS}(f)]$, where $G(f)$ is the Wiener filter. In a more general form, the Wiener filter can incorporate edge restoration in the same process. However, this filter requires that both NPS(f) and CPS(f) be constant in all regions of the image (ie, that both signal and noise processes be stationary). The fact that the tissue contrast varies widely with respect to fine detail and that noise varies with exposure limits the utility of any stationary filter and greatly complicates radiographic noise reduction.

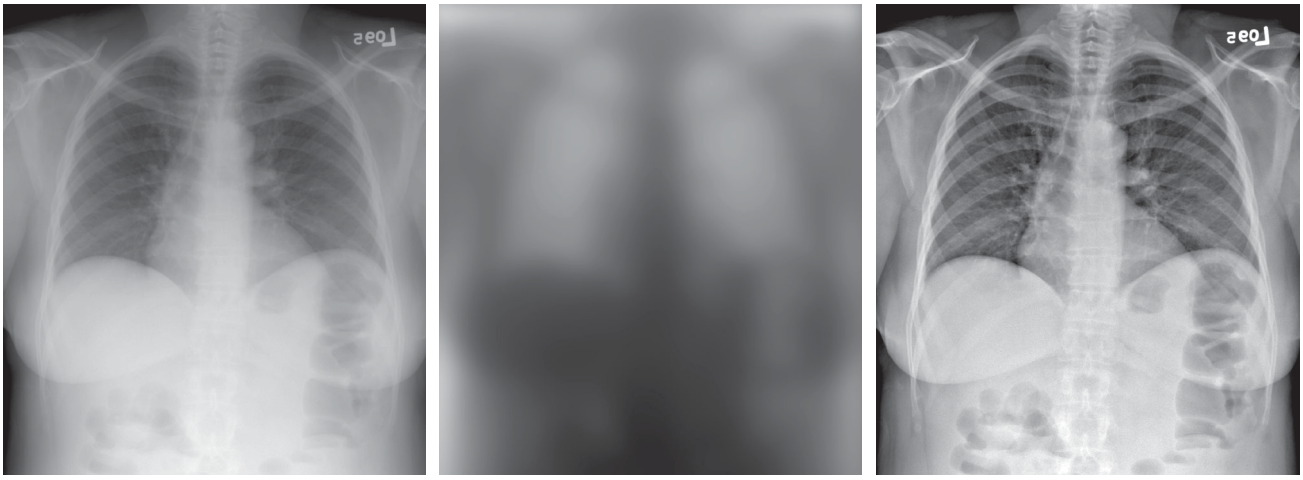

a. **b.** **c.**

Figure 4. **(a)** Digital radiograph of the chest obtained with a general-purpose CR screen by using no display processing. To display the wide range of raw image values, a wide-latitude gray-scale rendition has been used that results in poor tissue contrast. **(b)** Unsharp mask image derived from the chest image in **a** with the gray scale reversed. **(c)** Chest image in **a** with contrast enhancement based on the unsharp mask of **b**. The unsharp mask values are used to adjust the raw image values so that the image may be displayed with a narrow-latitude gray-scale rendition, resulting in improved tissue contrast. An equivalent photographic process would use the unsharp mask as illustrated to illuminate the original radiograph and make a high-contrast copy.

Adaptive noise reduction processes attempt to locally filter the image in regions where the tissue contrast has little fine detail. In regions containing sharp edges, fine detail, or other structures producing high-frequency components, the noise reduction is constrained and the detail preserved. The Lee filter is well known as a relatively simple edge-preserving filter that uses an estimate of the locally measured variance to control a convolution filter with a small-area kernel (17). Other adaptive approaches have been reported for other applications, including adaptive Wiener filtering (18). Noise reduction processes are difficult to successfully implement because the goals of reducing noise and preserving resolution are opposed.

The ability of noise reduction techniques to improve visual performance has been the subject of much debate. Because the human visual system can effectively recognize target patterns in the presence of noise, it is not necessarily true that a reduction in noise amplitude will improve detection performance. Moreover, if the noise texture is made coarser and if the filtered noise has a power spectrum similar to the target objects, the noise reduction process may be deleterious. Nonetheless, effectively applied adaptive noise reduction is likely to be of value with respect to improving the conspicuity of subtle features.

MATCHED LATITUDE

For screen-film systems, the H&D curve is selected to provide good contrast in the primary region of interest and acceptable latitude. For some views, this is not possible, and either contrast or latitude is compromised. For a posteroanterior chest view, if the latitude is sufficient to demonstrate mediastinal tissue structures, the lung tissues appear with low contrast. For lateral spine views, the contrast of the lumbar vertebral bodies may be good, but the posterior facets have insufficient exposure, and the thoracic spine elements have excessive exposure. Obtaining the proper latitude in an individual exposure is further compromised because most departments use only two or three screen-film systems (chest, general, and detail). With a large number of body parts and views for patients of varying size, the latitude can only match the average requirements.

The exposure recognition processes used to specify the gray-scale rendition allow latitude to be specified differently for each image obtained. With most systems, the operator specifies the body part and view prior to exposure. These entries can then be used to select the latitude of the I_{raw} values when generating the VOI LUT. When using a semiautomatic specification, the LUT values are automatically aligned with the histogram of I_{raw} values, but the LUT width (ie, latitude) is selected from a table by using the body part and view information. Alternatively, fully automatic specifications determine the width and level, as was described in the exposure recognition section. In general, exposure recognition processes allow greatly improved specification of the gray-scale latitude. With semiautomatic methods, the average exposure range associated with each view can be tabulated. With automatic methods, the latitude is adjusted for variations in the size of the subject. In practice, automatic methods have been limited to specific views, such as the posteroanterior chest.

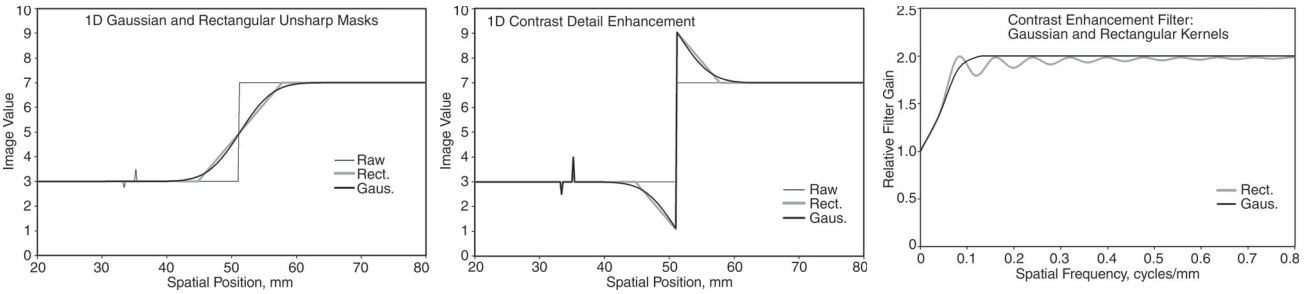

a. **b.** **c.**

Figure 5. **(a)** Blurring of raw image values to obtain an unsharp mask with a one-dimensional *(1D)* line of data crossing a sharp edge. A rectangular smoothing kernel (*Rect*; 16-mm width) with constant kernel weights produces a linear transition at the edge. A Gaussian smoothing kernel (*Gaus*; 16-mm width at 0.27 of the maximum) produces a smoothly varying transition. The fine detail structures seen in the raw data at left do not appear in the unsharp mask data. **(b)** Detail contrast enhancement based on an unsharp mask can be scaled so that the resultant image has the same values for low-frequency components (ie, the same latitude), but the contrast of edges and the fine detail are amplified. This is illustrated using the one-dimensional *(1D)* unsharp mask example from **a**. Note the smoothly varying overshoot at the edge that results from a Gaussian kernel *(Gaus)*. The detail contrast enhancement of the fine detail at the left is about twice that seen in the original data in **a**. **(c)** Enhancement of image components as a function of spatial frequency for the two examples of **b**. By using scaling to preserve latitude, the low frequencies are amplified with a gain near 1.0. Amplification increases with frequency to a gain of 2.0, in order to enhance detail contrast. For the process with the rectangular kernel *(Rect)*, ringing of the amplification is seen. In comparison, the process with the Gaussian kernel *(Gaus)* produces amplification that varies smoothly with spatial frequency.

CONTRAST ENHANCEMENT

Digital radiographs rendered with large latitude have poor contrast. Contrast enhancement processes are able to greatly improve the contrast of local tissue structures without altering the global gray-scale characteristics of the image. Image processing methods are used that maintain the low-spatial-frequency components of the image that are responsible for the average brightness in large regions while increasing the components with intermediate and high frequency that are responsible for detail contrast. Contrast enhancement processes result in both high contrast and wide latitude in a manner that is not possible with screen-film radiography.

The classical approach for contrast enhancement is the unsharp mask method. A blurred representation of the image is first prepared. This is then subtracted from the image to reveal the detail contrast. The two are then combined with appropriate weighting to obtain an enhanced image (Fig 4). The method originated as a photographic process in which a blurred negative is placed in contact with a positive film to diffusely increase the light transmission in dark regions. A high-contrast copy of the film is then made. This method has been commonly used to prepare prints for publication[5] and was described in 1981 as a method to improve chest radiographs (19).

Fuji Medical Systems introduced unsharp mask processing of digital radiographs on their early CR systems (20,21). By using appropriate weighting to diffusely increase low I_{raw} values and decrease high values, the range of values is compressed, allowing the use of a narrow-latitude gray-scale rendition. The method is referred to as dynamic range control; however, the purpose is to permit increased contrast. Numerous enhancements to this method have subsequently been reported and are used in commercial systems (22–25). These approaches use varying numeric methods to obtain good control of the enhancement response in relation to spatial frequency.

The specific manner is which enhancement is applied in relation to spatial frequency affects the appearance of tissue contrast in enhanced images, particularly at boundaries with a large change in the image value. At this boundary, all methods produce an artifact with a gradual short-range shift in image values. This response can be considered in terms of the shape of a convolution kernel used to blur the original image to obtain an unsharp mask (Fig 5a). Early methods used large kernels (1–4 cm) having constant values that caused a linearly varying transition at edges (Fig 5b). The frequency response for such a kernel has an undesirable oscillating response that can cause excessive amplification of certain tissue patterns. In comparison, if the kernel values are derived from a Gaussian function, the frequency response monotonically increases in a well-behaved manner (Fig 5c). Modern methods use multiscale and multifrequency processing methods that can be rapidly applied to achieve a well-behaved enhancement.

DISCUSSION

For each view of each body part, processes for noise reduction, edge enhancement, contrast enhancement, segmentation, exposure recognition, and gray-scale

[5] In 1972, logEtronics (Springfield, Va) patented a method to make photographic negatives of medical radiographs with unsharp masking (U.S. patent 3,700,329). A cathode-ray tube was used to illuminate the radiograph with a blurred mask. The multidodge system is now sold by Egoltronics (Baker, WVa).

rendition need to be specified and applied. Noise reduction is often done first because NPS(f) and its relation to exposure are known for the raw data. Edge restoration and contrast enhancement can often be done in combination by using convolution or frequency filtering processes. The gray-scale rendition is typically applied last so that it can be sent as a separate VOI LUT when possible.

Overall, these processes require specification of a large number of control parameters. Noise reduction may use several parameters to adjust adaptation and tissue contrast sensitivity. Edge enhancement may use several parameters to describe MTF shape, high-frequency reduction, and overall amplitude. Contrast enhancement may use several parameters to describe the effective blur width and the overall gain. Gray-scale rendition may use several parameters to select a curve shape and control the latitude. These numerous parameters need to be specified for each view of each body part that the system may examine. Because this process involves specification of about 100 parameter sets, considerable effort is required to develop systems with effective display processing.

When done properly, digital radiographic processing can produce dramatic improvements in image quality. However, when done improperly, the results can be frustrating and disappointing. The industry is presently challenged to implement robust methods that can achieve good results on all views of all body parts, even for extreme subject size or unusual anatomic presentations. Such optimization will continue to require close collaboration between medical centers and commercial developers.

References

1. Vuylsteke P, Dewaele P, Schoeters E. Optimizing computed radiography imaging performance. In: Frey DG, Sprawls P, eds. The expanding role of medical physicists in diagnostic imaging. Madison, Wis: Advanced Medical, 1997; 107–152.
2. National Electrical Manufacturers Association. Digital imaging and communications in medicine (DICOM) part 14: gray-scale standard display function. Rossyln, Va: National Electrical Manufacturers Association, 2003.
3. National Electrical Manufacturers Association. Digital imaging and communications in medicine (DICOM) part 3: information object definitions. Rossyln, Va: National Electrical Manufacturers Association, 2003.
4. Barski LL, Van Metter R, Foos DH, et al. New automatic tone scale method for computed radiography. SPIE Proc 1998; 3335:164–178.
5. Luo J, Senn RA. Collimation for digital radiography. SPIE Proc 1997; 3034:74–85.
6. Senn R, Barski L. Detection of skin line transition in digital medical imaging. SPIE Proc 1997; 3034:1114–1123.
7. Dewaele P, Ibison M, Vuylsteke P. A trainable rule-based network for irradiation field recognition in Agfa's ADC system. SPIE Proc 1996; 2708:72–84.
8. Takeo H, Nakajima N, Ishida N, et al. Improved automatic adjustment of density and contrast in FCR system using neural network. SPIE Proc 1994; 2163:98–109.
9. Gur D, Fuhman CR, Feist JH, Slifko R, Peace B. Natural migration to a higher dose in CR imaging (abstr). Presented at the Eighth European Congress of Radiology, Vienna, Austria, September 12–17, 1993; abstract 154.
10. Chan HP, Doi K, Metz CE. Digital image processing: effects of Metz filters and matched filters on detection of simple radiographic objects. SPIE Proc 1984; 454:420–432.
11. Metz CE. A mathematical investigation of radioisotope scan image processing. PhD dissertation. University of Pennsylvania, Philadelphia, Pa, 1969.
12. Barrett HH, Swindell W. Radiological imaging: the theory of image formation, detection, and processing. New York, NY: Academic Press, 1981; 247.
13. Samei E, Flynn MJ. An experimental comparison of detector performance for computed radiography systems. Med Phys 2002; 29:447–459.
14. Samei E, Flynn MJ. An experimental comparison of detector performance for direct and indirect digital radiography systems. Med Phys 2003; 30:608–622.
15. Wiener N. Extrapolation, interpolation, and smoothing of stationary time series, with engineering applications. Cambridge, Mass: Cambridge Technology Press of the Massachusetts Institute of Technology, 1949.
16. Rabiner LR, Gold B. Theory and application of digital signal processing. Englewood Cliffs, NJ: Prentice-Hall, 1975.
17. Lee JS. Digital image enhancement and noise filtering by use of local statistics. IEEE Trans Pattern Analysis Machine Intell 1980; 2:165–168.
18. Hillery AD, Chin RT. Iterative Wiener filters for image restoration. IEEE Trans Signal Processing 1991; 39:1892–1899.
19. Sorenson JA, Niklason LT, Nelson JA. Photographic unsharp masking in chest radiography. Invest Radiol 1981; 16:529–530.
20. Kobayashi M. Image optimization by dynamic range control processing. In: Proceedings of the IS&T 47th annual conference. Springfield, Va: Society for Imaging Science and Technology, 1993; 695–698.
21. Ishida M. Digital image processing: Fuji computed radiography technical review no. 1. Tokyo, Japan: Fuji Medical Systems, 1993.
22. Vuylsteke P, Schoeters E. Multi-scale image contrast amplification (MUSICA). SPIE Proc 1994; 2167:551–560.
23. Ogodo M, Hishinuma K, Yamada M, et al. Unsharp masking technique using multi-resolution analysis for computed radiography image enhancement. J Digit Imaging 1997; 10: 185–189.
24. Lure FYM, Jones PW, Gaborski RS. Multi-resolution unsharp masking technique for mammogram image enhancement. SPIE Proc 1997; 2710:830–839.
25. Van Metter RL, Foos DH. Enhanced latitude for digital projection radiography. SPIE Proc 1999; 3658:468–483.